Observations and Modeling of Ionospheric Disturbances Triggered by Rockets

*Charles Lin[1], Chia-Hung Chen[1], Mitsuru Matsumura[2], Jia-Ting Lin[1]

1.Department of Earth Science, National Cheng Kung University, 2.National Institute of Polar Research, Research Organization of Information and Systems

This study presents two-dimensional structure of disturbances wave signatures in ionospheric electron density resulting from the rocket transit using the rate of change of the total electron content (TEC) derived from ground-based GPS receivers around Japan and Taiwan. From the TEC maps constructed for the recent five rocket launches around East Asia region, features of the V-shape shock wave fronts in TEC perturbations are prominently seen. These fronts, with period of 100-600 sec, produced by the propulsive blasts of the rockets appear immediately and then propagate perpendicular outward from the rocket trajectory with supersonic velocities between 800-1200 m/s for both events. Following the initial shock wave feature, various disturbances waves in TEC are seen. Twenty minutes after the rocket transits, delayed electron density perturbation waves propagating along the bow wave direction appear with phase velocities of 800-1200 m/s. According to the propagation character, these delayed waves may be generated by rocket exhaust plumes at earlier rocket locations at lower altitudes. The upward propagating disturbance waves due to exhaust plumes from lower altitude are also reconstructed by comprehensive model calculations.

Keywords: Ionospheric Disturbance Waves, Rocket Exhaust

Study of dynamics of tsunami ionospheric hole from geomagnetic observation

*Yuto Tomida[1], Tatsuya Kanaya[1], Masashi Kamogawa[1], Makoto Uyeshima[2]

1.Department of Physics, Tokyo Gakugei University, 2.Earthquake Research Institute, The University of Tokyo

Approximately several minutes after the occurrence of the mainshock of the M9.0 off the Pacific coast of Tohoku Earthquake on 11 March 2011, various geo-electromagnetic phenomena was in Japan and even in the magnetic conjugate point of Japan (i.e. Australia) through magnetic field lines as a field align current. In this paper, we show electromagnetic phenomena after the 2011Tohoku earthquake in the ionosphere such as tsunami ionospheric hole, seismo-field align current, Rayleigh-wave-induced ionospheric arc current, and seimic- ionospheric ring current (SRIC). SRIC was highly related to tsunami ionospheric hole observed by GPS-TEC.

Keywords: Magnetic field, Earthquake, Tsunami, Tsunami ionospheric hole

Smal-scale variations of ionospheric TEC observed with a hyper-dense GNSS receiver network

Yuji Takeda[1], Naoki Ito[1], *Toshitaka Tsuda[1], Atsuki Shinbori[1]

1.Research Institute for Sustainable Humanosphere

We employ the GNSS meteorology to estimate TEC (total electron content) and PWV (Precipitable Water Vapor) in the ionosphere and troposphere, respectively, from the propagation delay of GNSS signal. We established a hyper-dense GNSS receiver network in Uji using 7 to 15 receivers with 1-2 km spacing. We found difference of PWV in 10 km was 3-10 mm during a heavy rain. For a future system, we use inexpensive single-frequency (SF) receivers. Because SF receiver cannot eliminate the ionospheric delay, we interpolate the delay referring to the results from nearby dual frequency (DF) receivers.
We investigated ionospheric delay by the Uji network, taking advantages of QZSS(Quasi-Zenith Satellite System) that gives signals at high elevation angles. Effects of ionospheric perturbations due to sun-rise/sun-set and a geomagnetic storm were small, so they do not give serious influence on PWV. During a travelling ionospheric disturbance, a wavy structure with a horizontal scale of several tens km was recognized. These ionospheric effects can be compensated by a linear or quadratic interpolation.
We corrected the ionospheric delay on SF observation with 30 sec sampling with SEID developed by GFZ. The resulting error of PWV compared with DF solution was about 1.50 mm in RMS. By improving the time resolution of the interpolation from 30 to 1sec, error is suppressed by about 70%.

Keywords: GNSS meteorology, hyper-dense GNSS receiver netwrok , PWV (precipitable water vapor), TEC (total electron content), ionospheric propagation delay

Observation of mid-latitude sporadic E over North America by GNSS-TEC

*Takato Suzuki[1], Masato Furuya[2], Kosuke Heki[2], Jun MAEDA[3]

1.Hokkaido University, 2.Faculty of Science, Hokkaido University, 3.Hokkaido University Library

Maeda and Heki. (2014) succeeded in capturing sporadic E (Es) over Japan two-dimensionally, using the observation of Global Navigation Satellite System - Total Electron Content (GNSS-TEC). We aimed to capture Es over the western coast of North America where there is mid-latitude same as Japan and GNSS stations are dense.
First, we chose the dates whose critucal frequencies of Es (foEs) were more than 12 MHz at Disisonde in Pt. Arguello (lat: 34.8, lon: 239.5) in the morning and noon in 2006 through 2015 from May to August. Second, we made GNSS-TEC maps.
We succeeded in capturing Es over America and indicated that a strong Es appeared also at different longitude can be captured by GNSS-TEC. Es observed this time had E-W direction slope. It is though that this reflects E-W wind shear.

Keywords: Sporadic E, GNSS-TEC

Generating mechanism of Medium-Scale Traveling Ionospheric Disturbance using a GPS network in Alaska

Takuya Mizoguchi[1], *Yuichi Otsuka[1], Kazuo Shiokawa[1], Michi Nishioka[2], Takuya Tsugawa[2]

1.Institute for Space-Earth Environmental Research, Nagoya University, 2.National Institute of Information and Communications Technology

In our previous study, using global positioning system (GPS) data taken from GPS receivers in Alaska in 2012 and in Northern Europe in 2008, we investigated two-dimensional maps of total electron content (TEC) perturbations with a time resolution of 30-s and a spatial resolution of 80 km80 km in longitude and latitude to disclose statistical characteristics of Medium-Scale Traveling Ionospheric Disturbance (MSTID) at high-latitudes. Based on the statistical characteristics of MSTID at high-latitudes, we have found that the observed MSTIDs are divided into three groups: 1. daytime MSTID occurring in winter in Alaska and Northern Europe, 2. nighttime MSTID occurring in summer in Northern Europe, and 3. dusk MSTID occurring in winter in Alaska. The daytime and nighttime MSTIDs at high-latitudes are consistent with those observed at mid-latitudes in terms of local time dependence of their occurrence rate and propagation direction, but the dusk MSTID has not been observed at mid-latitudes. In this presentation, we focus on the generation mechanisms of the dusk MSTID which occurs in winter in Alaska by investigating whether the MSTID is generated by the same mechanism as those at mid-latitudes, from the view point of electrodynamics and neutral atmosphere dynamics.
At first, we consider the generation mechanisms of MSTIDs from a standpoint of electrodynamics. We find that vertical component of plasma motion is restricted and amplitude of TEC perturbation by $E \times B$ drift is small because magnetic field line is close to vertical at high-latitudes. We discuss the theory that polarization electric fields in sporadic E layer play an important role in generating that MSTID through E- and F-region coupling process. According to this theory, MSTID occurs simultaneously at conjugate points in the northern and southern hemisphere connected by geomagnetic field lines. However, the observational results show that local time dependence of MSTID in Alaska and New Zealand is different. Therefore, we conclude that MSTID observed dusk in winter in Alaska could not be generated by electrodynamics.
Secondly, we research whether the dusk MSTID is generated by atmospheric gravity waves (AGWs) or not. Previous studies suggest that MSTIDs could be caused by AGWs excited by auroral activities. In this study, we have investigated various indicators which could represent auroral activity, such as ROTI (Rate of TEC change Index), AE index and Kp index. We have found that there is no clear correlation between occurrence rate of MSTID and these indices.
To determine the location of the AGW sources, we apply the backward ray tracing method of AGWs. Results of a backward ray tracing analysis show that the AGWs can reach ionosphere from an altitude of 10 km in 24 of 34 events. In a few cases, AGWs traced backward from the ionosphere reach a critical level at an altitude of the stratosphere. This result indicates a possibility that AGWs excited by polar vortex in the stratosphere propagate to the ionosphere and generate the MSTIDs. We need further studies about source region of AGWs to reveal generation mechanisms of MSTIDs at high-latitudes.

Keywords: ionosphere, traveling ionospheric disturbance, GPS

Spectral analyses of resonance scattering of Sr and Ba for determination of thermospheric neutral wind

*ko saito[1], Yoshihiro Kakinami[1], Masa-yuki Yamamoto[1]

1.Kochi Uniersity of Technology

1. Introduction: We developed a measurement technique for the wind velocity profile in the thermospheric rarefied atmosphere by Lithium(Li) releases from sounding rockets in cooperation with JAXA and NASA. We observed barium (Ba) and barium ion (Ba^+) released by sounding rocket in Norway in November, 2014, and observed the thermospheric neutral wind and the ion drift at an altitude range of 150~400 km. In the future, Japan is going to carry out the similar measurement using strontium (Sr), and the experiment using the Sr ejection system was performed as a preliminary experiment on ground in Gunma prefecture in September, 2014. Here we report both of the results of the spectrum analyses from the observed images of Sr and Ba in order to verify the released components of Ba and Sr.

2. Spectrum analysis: The spectrum observation method of this experiment in Norway was observation of spectrum images by a camera (Nikon D700) with an attached diffraction grating (500 line/mm) without a slit to the front of lens. The spectrum observation for the Sr preliminary experiment on ground was performed using a video camera (SONY DCR-PC101) attached to the same diffraction grating with a slit as well as a fiber input type spectrophotometer. We analysed the brightness distribution of the 1st order spectrum section using a developed image processing software by using IDL (Interactive Data Language) language and made a brightness level in each pixel on the image. Then, photographed bright-line spectrum of the Ar gas by a small Ar discharge tube was used for calibration of the spectrum camera and the spectrum video camera. The Ar lines are used as a basis of wavelengths for calibration. We acquired multiple Ar line wavelengths to calibrate calibrated the brightness spectrum distribution of Sr emission on ground as well as Ba and Ba^+ resonance scattering light in thermosphere. In addition, the spatial integrated spectrum strength obtained by the fiber input type spectrophotometer was also used for Sr measurement.

3. Spectrum analysis and discussion: From the spectrum analysis of the images taken at the rocket experiment in Norway, emission spectrum of wavelengths at 455 nm, 557 nm and 610 nm - 661 nm was confirmed. The wavelengths were fixed as the wavelengths of the documented Ba^+ and the Ba emissions at 455 nm and 553 nm. From the spectrum analysis, we can confirm an emission wavelength at 460 nm obtained at the Sr ground experiment as 460.7 nm emission which is documented as the Sr spectrum line. We could clearly detect Sr 460.7 nm by integrating multiple spectrum sections on an image. From the data analysis for the spectrophotometer measurement, we confirmed a spectrum of iron (Fe) and aluminum (Al) at 635 nm, 644 nm and 656-659 nm as well as oxygen (O_2) at of 668 nm –671 nm, suggesting the effect by the thermite reaction in case of the Sr release.

4. Conclusion: We confirmed the emissions at the of wavelengths 455 nm and 557 nm from the sequential spectrum images which the sounding rocket experiment in Norway provided and those were fixed as Ba^+ and Ba, thus Ba release and ionization were confirmed. In addition, it is concluded that when we confirm a brightness peak at 460.7 nm by the two types of spectrum data obtaind by the ground measurement, Sr release and emission was confirmed.

Keywords: strontium, resonance scattering, thermosphere

Numerical simulation of magnetic field variation associated with equatorial plasma bubble

*Tatsuhiro Yokoyama[1], Claudia Stolle[2]

1.National Institute of Information and Communications Technology, 2.GeoForschungsZentrum Potsdam, Germany

Equatorial plasma bubble (EPB) is a well-known phenomenon in the equatorial ionospheric F region. As it causes severe scintillation in the amplitude and phase of radio signals, it is important to understand and forecast the occurrence of EPB from a space weather point of view. The development of EPB is known as a evolution of the generalized Rayleigh-Taylor instability. We have developed a new 3D high-resolution bubble (HIRB) model for EPB and presented nonlinear growth of EPB which shows very turbulent internal structures such as bifurcation and pinching. Recently, it has been reported that high-resolution magnetometer onboard low Earth orbit satellites such as CHAMP and Swarm can detect small-scale magnetic field perturbation associated with EPBs. It is interpreted as the diamagnetic effect produced by pressure gradient-driven current, and field-aligned current flowing along the walls of EPBs. We have upgraded the 3D numerical simulation model by removing the equipotential magnetic field assumption so that 3D current distribution can be calculated. The magnetic field variations produced by the current associated with EPBs are consistent with the in situ observations and expected physical models. It is also important for internal magnetic field modeling because such magnetic field variations are comparable to that of the lithospheric contribution.

Keywords: plasma bubble, magnetic field, simulation, CHAMP satellite

Preliminary report of a sounding rocket experiment to elucidate electron heating in the Sq current focus
- Observations of DC Electric field and VLF band plasma wave -

*Yuka Ataka[1], Keigo Ishisaka[1], Takumi Abe[2], Makoto Tanaka[3], Atsushi Kumamoto[4], Akimasa Yoshikawa[5], Hiroki Matsushita[5]

1.Toyama Pref. Univ., 2.ISAS/JAXA, 3.Tokai Univ., 4.Tohoku Univ., 5.Kyushu Univ.

The Sq current system occurs in the lower ionosphere in the winter daytime. The center region of the Sq current system is appeared the specific plasma phenomenon such as electron heating, strong electron density disturbance. S-310-44 sounding rocket equipped with each scientific instrument and is launched toward the center of the Sq current system. The rocket observe the physical quantity for the investigation of the specific phenomenon. As similar experiment, S-310-37 sounding rocket had been performed in the past, however it was not possible to observe the electric field component of the magnetic field-aligned direction. It is one of the reasons that the photo electron caused by the sunlight that is irradiated to the rocket body, and affect the electric field observations. It is very difficult to remove the influence of the photo electron from the observed data. If it is possible to put the electrode of the electric field sensor outside of the region where there become the photo electron around the rocket body, the influence of the photo electron can be reduced. Therefore, the antennas need a length as long as possible to observe the electric field. Accordingly, the antennas of S-310-44 sounding rocket is 4m tip-to-tip that is twice as length than the antennas of S-310-37 sounding rocket. The purpose is to reduce the influence of the photo electron moreover to measure the electric field more accuracy.
It was carried out the S-310-44 sounding rocket experiment at Uchinoura Space Center (USC) at 12:00 LT on January 15, 2016. This rocket passed through near the center of the Sq current system. In addition, scientific observation instruments that are equipped on the rocket also operated normally. In Electric Field Detector (EFD), the antennas have started extension after 67 seconds (altitude 81km) from launch. After 81 seconds (altitude 97km) the full extension, the observation was started. There was not seen the effect by photo electron in observed the electric field data. Here we analyze the electric field data obtained in the S-310-44 sounding rocket. And we describe the derivation result of the electric field that it is important for the investigation of the Sq current system generating mechanism.

Keywords: electric field , sounding rocket experiment, Sq current system

Sounding rocket experiment to clarify electron heating phenomena in the Sq current focus - Plasma wave observation -

*Atsushi Kumamoto[1], Keigo Ishisaka[2], Yuka Ataka[2], Takao Takahashi[3], Makoto Tanaka[3], Takumi Abe[4]

1.Department of Geophysics, Graduate School of Science, Tohoku University, 2.Toyama Prefectural University, 3.Tokai University, 4.JAXA

In order to clarify electron heating phenomena in the center of Sq current focus in the winter ionosphere, the sounding rocket experiment S-310-44 was launched at 21:00 UT (12:00 JST) on January 15, 2016 at Uchinoura Space Center (USC). Plasma Wave Monitor (PWM) onboard the S-210-44 was successfully measured plasma waves in a frequency range from 300 Hz to 22 MHz along the rocket trajectory with apex altitude of 160 km, which is also confirmed to be near the Sq current focus by using data from magnetometer chain on the ground. The AC electric field was picked up with two antenna elements (EFD-ANT-1 and 2), and respectively amplified by two preamplifiers (EFD-Pre-1 and 2) of the Electric Field Detector (EFD). Then, two signals were fed to two PWM inputs (PWM-HF and PWM-VLF), respectively. The signal fed to PWM-HF was sampled at 81.92 MSPS and converted to spectrum in a frequency range from 20 kHz to 22 MHz with 400 frequency steps. The signal to PWM-VLF was sampled at 81.92 kSPS and converted to spectrum in a frequency range from 300 Hz to 20kHz with 400 frequency steps. These spectra were obtained every 125 msec. EFD antenna elements were stored on the ground and deployed at altitude of 85 km. So the altitude range from 85 km to 160 km are covered in ascent, and all altitude range below 160 km are covered in descent.
During the flight, the following phenomena were identified: (1) Harmonic emissions of lower hybrid resonance (LHR) were found in a frequency range from several hundred Hz to several kHz. Their frequencies changes depending on the ambient plasma density and likely on the ion compositions. They are enhanced at altitude around 100 km in ascent but not enhanced at the same altitude in descent. (2) Upper hybrid resonance (UHR) waves were not found in a frequency range around several MHz. In most previous sounding rocket experiment, UHR waves were found in altitude range higher than 200 km, and masked at altitude below 200 km by the artificial radio waves from the ground. In this experiment, the artificial radio waves were not so intense to mask the other emissions.
The LHR waves can be generated by various energy inputs. Baker et al. [2000] reported that LHR emissions were found in the sounding rocket experiment, and suggested that they are caused by the whistler waves from the thunderstorms on the ground. The enhancement of LHR only in ascent suggests that the energy source of LHR wave is localized in narrow area in E region of the ionosphere. Through the comparisons with data from the other instruments onboard the S-310-44 such as electron density and temperature (FLP), DC and AC electric fields (EFD), and currents (MGF), we will be able to discuss the energy source of the observed LHR waves in more detail.

Keywords: The sounding rocket experiment S-310-44, Sq current focus, Plasma wave observation, Lower hybrid resonance wave

Preliminary report of a sounding rocket experiment to elucidate electron heating in the Sq current focus
- Observations of thermal electron energy distribution -

*Takumi Abe[1], Keigo Ishisaka[2], Atsushi Kumamoto[3], Makoto Tanaka[4], Takao Takahashi[4], Hiroki Matsushita[5], Akimasa Yoshikawa[5]

1.Japan Aerospace Exploration Agency Institute of Space and Astronautical Science Department of Solar System Sciences, 2.Toyama Prefectual University, 3.Tohoku University, 4.Tokai University, 5.Kyushu University, Faculty of Sciences

Sounding rocket observations in Japan suggest that the electron temperature profile occasionally exhibits the local increase by several hundred K at 100-110 km altitudes at 1100-1200 LT in winter. Detailed study of the temperature profiles indicates that such an increase is closely related to the existence of Sq current focus, because it becomes more significant when the measurement is made near the center of Sq focus. In order to understand a general feature and to investigate a generation mechanism of this unusual phenomena, a sounding rocket experiment was carried out.
In this experiment, “S-310-44” rocket equipped with a suite of five science instruments was launched from Uchinoura Space Center at 12:00 JST on January 16, 2016 after being convinced that the Sq current was approaching to the planned rocket trajectory. In this presentation, we will focus on the energy distribution of thermal electrons and electron temperature obtained from FLP (Fast Langmuir Probe) instrument onboard the rocket.
In the FLP instrument, a small AC voltage with a frequency of 2 kHz was superimposed on a triangular voltage bias with an amplitude of 3 V. It is possible to estimate energy distribution from the amplitude of the second harmonic component of 2 kHz in the probe current. Moreover, the electron temperature can be estimated from the electron energy distribution, when the energy distribution is considered to be *Maxwellian*. Another function of the FLP is to be able to provide a small-scale (< 1 m) electron density perturbation, which can be estimated from the electron saturation current provided by a fixed bias spherical probe installed on the rocket axis.
During this experiment, a group of Kyushu University has continuously measured the geomagnetic field on the ground to estimate exact position of Sq current focus, because it is required for the rocket trajectory to be close enough to the current focus. Their analysis about the magnetometer data suggests that *in-situ* observations of electrons, magnetic and electric fields were conducted in the distance of 200 to 300 km from the current focus.
The FLP successfully made its measurement during both upleg and downleg of the rocket flight. Observations of the energy distribution suggest that the electron temperature increased by about 200 K with respect to the background in the altitude range from 100 to 110 km. It is also significant that the observed energy distribution unlikely seems *Maxwellian* distribution and sometimes exhibits a possible existence of *non-Maxwellian* component in the high electron temperature region. Power spectrum analysis of the electron current by the fixed bias probe indicates that the amplitude in the frequency range of several hundred Hz increased at the E region altitude. In particular, it is remarkable that the strong electron density perturbation was observed in the broad frequency range at altitudes from 95 to 110 km. In this presentation, we give a report on the preliminary analysis of the thermal electron measurements in more detail.

Keywords: Sq current system, sounding rocket, electron heating

Variation of equivalent current system representing geomagnetic Sq variation in the period of 1980-2010

*Masahiko Takeda[1]

1.Data Analysis Center for Geomagnetism and Space Magnetism, Graduate School of Science, Kyoto University

Spherical harmonics analysis was performed for the geomagnetic Sq field from 1980 to 2010 for every universal hour on each day. Solar activity dependence of the total Sq currents was confirmed, and variation in each solar cycle was also reflected in the total current intensity.
More detailed features of the long trend of the Sq field will be discussed in the presentation.

Keywords: geomagnetic daily variation,, equivalent current system, secular variation, solar activity

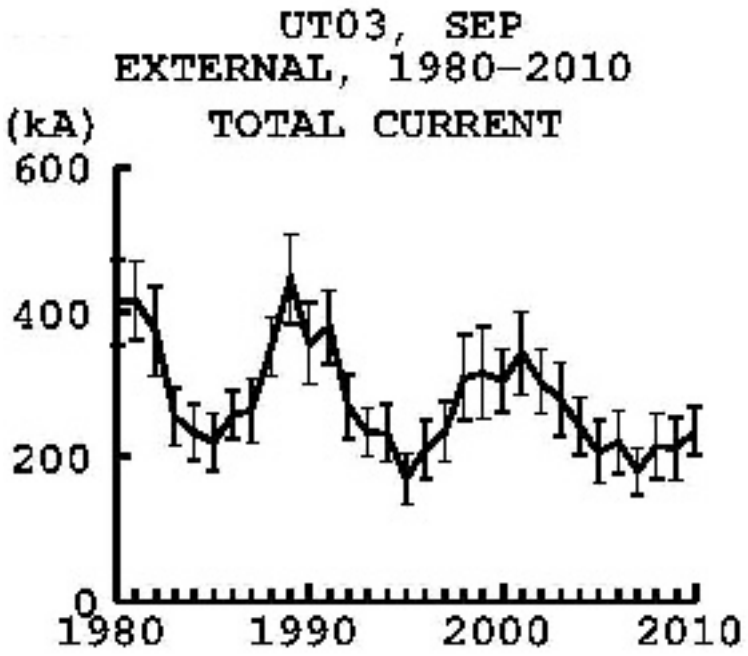

Horizontal Distributions of Sprites and the Relation to Parent Lightning Discharges Derived from JEM-GLIMS Nadir Observations

*Mitsuteru Sato[1], Toru Adachi[2], Tsuyoshi Sato[3], Tomoo Ushio[4], Takeshi Morimoto[5], Makoto Suzuki[6], Atsushi Yamazaki[6], Yukihiro Takahashi[1]

1.Faculty of Science, Hokkaido University, 2.Meteorological Research Institute, 3.Department of Cosmosciences, Hokkaido University, 4.Graduate School of Engineering, Osaka University, 5.Faculty of Science and Engineering, Kinki University, 6.ISAS/JAXA

JEM-GLIMS carried out ~3-years nadir observations of lightning discharges and lightning-producing transient luminous events (TLEs) at the ISS. In this period, JEM-GLIMS succeeded in detecting 8357 lightning events and 699 TLEs. From the detailed data analyses, 42 and 508 events in 699 TLEs are confirmed to be sprites and elves, respectively. It is found that the delay time of the sprite occurrence from the parent lightning occurrence is ~1 ms in all the sprite events (i.e., short-delayed sprites) and that the sprite emissions occurred above the parent lightning emissions. However, the exact location of the sprite emissions was slightly displaced from the peak location of the parent lightning emissions, which is regarded as the return stroke point. We statistically estimated the displacement and found that the median and average values are 13.6 km and 13.3 km, respectively. This result is consistent with the pervious report of *Lu et al.* [JGR, 2013], who suggested that the short-delayed sprites tend to occur within 30 km from the return stroke point. At the presentation, we will show the characteristics of the horizontal distributions of sprites and discuss the possible mechanism of the displacement more in detail.

Keywords: Lightning, TLEs, ISS

Lower-thermospheric wind variations in auroral patches during the substorm recovery phase

*Shin-ichiro Oyama[1], Kazuo Shiokawa[1], Yoshizumi Miyoshi[1], Keisuke Hosokawa[2], Brenton J Watkins[3], Junichi Kurihara[4], Takuo T. Tsuda[2], Christopher T Fallen[3]

1.Institute for Space-Earth Environmental Research, Nagoya University, 2.University of Electro-Communications, 3.Geophysical Institute, University of Alaska Fairbanks, 4.Hokkaido University

Responses of the polar thermosphere and ionosphere to geomagnetic substorms have been widely investigated by many researchers. Representative mechanisms that may cause such variations are thermal energy dissipation by the Joule and particle heating processes and momentum transfer by the Lorentz force. The mechanisms and thermospheric/ionospheric responses have been studied by analyzing data mainly at the expansion phase or around the substorm onset. In contrast the substorm recovery phase has had little focus for most researchers. A motivation for this work is spontaneous and dramatically large variations of density, temperature, and dynamics in the thermosphere and ionosphere at the substorm recovery phase.
At the substorm recovery phase, measurements of the lower-thermospheric wind with a Fabry-Perot interferometer (FPI) at Tromsø, Norway found the largest wind variations in a night during appearance of the auroral patches. Taking into account magnetospheric substorm evolution of plasma energy accumulation and release, the largest wind amplitude at the recovery phase is a fascinating result because it is generally assumed that the energy dissipation at the recovery phase is smaller than that at expansion phase and onset. The results are the first detailed investigation of the magnetosphere-ionosphere-thermosphere coupled system at the substorm recovery phase using comprehensive data sets of solar wind, geomagnetic field, auroral pattern, and FPI-derived wind. This study used three events in November 2010 and January 2012, particularly focusing on the wind signatures associated with the auroral morphology, and found three specific features: (1) wind fluctuations that were isolated at the edge and/or in the darker area of an auroral patch with the largest vertical amplitude up to about 20 m/s and with the longest oscillation period about 10 minutes, (2) when the convection electric field was smaller than 15 mV/m, and (3) wind fluctuations that were accompanied by pulsating aurora. This approach suggests that the energy dissipation to produce the wind fluctuations is localized in the auroral pattern. Effects of the altitudinal variation in the volume emission rate were investigated to evaluate the instrumental artifact due to vertical wind shear. The small electric field values suggest weak contributions of the Joule heating and Lorentz force processes in wind fluctuations. Other unknown mechanisms may play a principal role at the recovery phase.

Keywords: aurora, thermosphere, Fabry-Perot interferometer, substorm recovery phase

Test observations by a frequency-tunable resonance scattering lidar

*Mitsumu K. Ejiri[1], Takanori Nishiyama[1], Takuo T. Tsuda[2], Makoto Abo[4], Katsuhiko Tsuno[3], Satoshi Wada[3], Takayo Ogawa[3], Takuya Kawahara[5], Takuji Nakamura[1]

1.National Institute of Polar Research, 2.The University of Electro-Communications, 3.RIKEN, 4.Graduate School of System Design, Tokyo Metropolitan University, 5.Faculty of Engineering, Shinshu University

The National Institute of Polar Research (NIPR) is leading a six year prioritized project of the Antarctic research observations since 2010. One of the sub-project is entitled the global environmental change revealed through the Antarctic middle and upper atmosphere. Profiling dynamical parameters such as temperature and wind, as well as minor constituents is the key component of observations in this project, together with a long term observations using existent various instruments in Syowa, the Antarctica (69S). As a part of the sub-project, we are developing a new resonance lidar system with multiple wavelengths and plan to install and operate it at Syowa, Antarctica. The lidar will observe temperature profiles and variations of minor constituents such as Fe, K, Ca^+, and aurorally excited N_2^+. The lidar system is being developed with trial and error in test observations of the metal atom and ion density and the MLT temperature profiles. The lidar will be installed at Syowa in Antarctica by the 58th Japan Antarctic Research Expedition (JARE 58). In this presentation, we will report current status of the system developments and discuss results of the test observations.

Keywords: resonance scattering lidar, Mesosphere Lower-Thermosphere Region, Temperature measurement, Metal atom, Metal ion

One night variation of horizontal phase velocity distribution of mesospheric gravity waves at Syowa

*Takashi S. Matsuda[2,1], Takuji Nakamura[1,2], Masaki Tsutsumi[1,2], Mitsumu K. Ejiri[1,2], Yoshihiro Tomikawa[1,2]

1.National Institute of Polar Research, 2.Graduate University for Advanced Studies

Gravity waves, generated in the lower atmosphere, can propagate to the mesosphere and the lower thermosphere, and transport great amount of energy and momentum, and release them at various altitude regions. Among many parameters to characterize gravity waves, horizontal phase velocity is very important to discuss vertical propagation and where the momentum is released. Near the mesopause region, OH and other airglow imaging has been used for investigating the horizontal structures of gravity waves for more than two decades. Although the huge amount of the image data has been observed at various observation sites all over the world, a time consuming manual procedure has been used for extracting horizontal propagation characteristics from airglow data. This causes difficulty in obtaining a global map of gravity wave characteristics in the mesopause region. Another important fact on the mesospheric gravity wave studies is that observations over the Antarctic region were quite rare despites a significant amount of gravity waves generated in this region.
Matsuda et al., 2014 developed new statistical analysis method for deriving horizontal phase velocity spectrum of gravity waves derived from airglow imaging data. It is suitable to not only deal with a large amount of data, but also reveal temporal variation of phase velocity spectrum. In this study, we obtained 9 horizontal phase velocity spectra every an hour at 1501-0000 on May 11 2013 at Syowa (69S, 40E). We compared these spectra with background wind using re-analysis data (MERRA) and MF radar data, and found that effect of wind filtering by critical level could not explain the temporal variation.

Keywords: Atmospheric gravity waves, Airglow imaging, Mesosphere

Long-term variation of horizontal phase velocity spectrum of mesospheric gravity waves observed by an airglow imager at Shigaraki : Comparison with tropospheric re-analysis data

*Daiki Takeo[1], Kazuo Shiokawa[1], Hatsuki Fujinami[1], Yuichi Otsuka[1], Takashi S. Matsuda[2], Mitsumu K. Ejiri[2], Takuji Nakamura[2], Mamoru Yamamoto[3]

1.Institute for Space-Earth Environmental Research Nagoya University, 2.National Institute of Polar Research, 3.Research Institute for Sustainable Humanosphere, Kyoto University

Atmospheric gravity waves (AGWs) generated in the lower atmosphere transport momentum into the upper atmosphere and release it when they break near the mesopause region. The released momentum drives global-scale pole-to-pole circulation in the upper atmosphere, causing global mass transport. The AGW propagation and its momentum transport depend on horizontal phase velocity of AGWs. There were many studies about the AGWs in the past by using radars, lidars and airglow imagers, and various AGW parameters such as wavelengths and phase velocities were studied. However, long-term (>10 years) variation of horizontal phase velocity spectrum of the mesospheric small-scale AGWs, which can be measured by airglow imagers, has not been studied yet.
In this study, we analyze the horizontal phase velocity spectrum of AGWs by using mesospheric 557.7-nm airglow images obtained at Shigaraki MU Observatory (34.8 deg N, 136.1 deg E) of Kyoto University over ~17 years from October 1, 1998 to July 26, 2015. We use 3-dimensional Fourier analysis procedures of airglow images proposed by Matsuda et al. (JGR, 2014), making it possible to analyze large amount of data.
Seasonal variations of propagation direction of AGWs was clearly identified (Spring : North-East and South-West, Summer : North-East, Fall : North-West, Winter : South-West). Several longer-term variations of direction / intensity were identified for each season with a time scale of several years. The power spectrum density of horizontal phase velocity changes with 7-8 years timescale in winter and 2-3 years in spring.
The east-west anisotropy (summer: eastward, winter: westward) of AGW propagation is probably caused by filtering of gravity waves due to mesospheric jet (summer: westward, winter: eastward) (e.g., Nakamura et al., EPS, 1999; Ejiri et al., JGR, 2003). However, north-south anisotropy (summer: northward, winter: southward) cannot be explained by mesospheric jet. Then we investigate the location of possible AGW sources relative to Shigaraki by using tropospheric re-analysis data about vertical flow velocity to understand the north-south anisotropy. There are regions of strong vertical velocities at south of Japan due to the Baiu seasonal rain front during summer and at north-east of Japan due to wintry low pressure during winter. Thus we consider that the north-south anisotropy of AGW propagation direction is due to the location of AGW sources in summer and winter.
Next, we investigated the relationships of longer-term variations of power spectrum density (PSD) of horizontal phase velocity of AGWs with tropospheric re-analysis data, NINO index, AO index and sunspot numbers particularly for summer and winter. There is a correlation between longer-term variations of PSD and tropospheric re-analysis data at south of Japan during summer and north-east of Japan during winter. These regions nearly correspond to the rain front in summer and the wintry low pressure in winter, as we described before. Thus we think more certainly that the north-south anisotropy of AGW propagation direction is controlled by the relative location of AGW sources. We could not find any clear correlations of PSD variations with NINO index, AO index and sunspot numbers.

Keywords: mesospheric gravity waves, horizontal phase velocity spectrum, long-term analysis, airglow imager, tropospheric re-analysis data

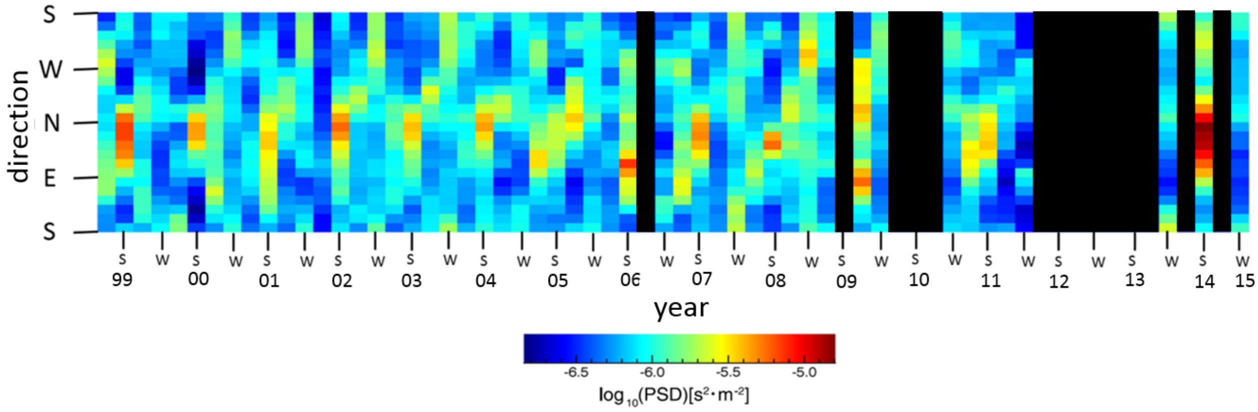

Variations in the reflection height in the lower ionosphere associated with typhoons using LF transmitter signals

*Hiroyo Ohya[1], Keisuke Asada[2], Fuminori Tsuchiya[3], Kazuo Shiokawa[4], Hiroyuki Nakata[1], Kozo Yamashita[5], Yukihiro Takahashi[6]

1.Graduate School of Engineering, Chiba University, 2.Faculty of Engineering, Chiba University, 3.PPARC, Graduate School of Science, Tohoku University , 4.Institute for Space-Earth Environmental Research, Nagoya University, 5.Department of Electrical Engineering, Salesian Polytechnic, 6.Graduate School of Science, Hokkaido University

So far, several studies for gravity waves caused by typhoons have been reported, although there are few studies for the lower ionosphere variations associated with typhoons using LF transmitter signals. In this study, we investigate variations of the D-region height associated with a typhoon of 11-20 June, 2012 using phase data of LF transmitter signals. There were two magnetic storms (minimum Dst values:-51 nT on 12 June and -71 nT on 17 June) in these dates. The propagation paths were Fukushima-Pontianak (PTK, Indonesia, 40 kHz) and Saga-PTK (60 kHz). We converted the phase data to reflection heights based on Earth-ionosphere waveguide mode theory. The period of the reflection height variations was analyzed by wavelet transform. The reference days were 23, 24, and 29 June, 2012, which were also geomagnetically quiet days. We excluded the periods of the reflection height variations seen in these reference days from the periods during the typhoon. In daytime during the typhoon, several solar flares were identified by the GOES X-ray flux. When the solar flares occurred, the reflection heights were largely decreased. Only nighttime data of the reflection height were analyzed because the duration of the gravity waves is expected to be several hours. As a result, the common periods of the reflection height over both propagation paths were 45.3 minutes on 15 June, 2012, and 76.1 minutes on 16 June. The duration of the periods was about 50 minutes in nighttime. In the two nights, medium-scale traveling ionospheric disturbances were not observed in the GPS-TEC data over Japan. The horizontal wavelengths were calculated from the onset time difference of the oscillations between the two propagation paths, and difference of the distance between the source location (the typhoon) and the two propagation paths. The horizontal wavelengths were estimated to be 483 -662 km for the 45.3 minutes and 1222 -1346 km for the 76.1 minutes. The horizontal wavelengths were comparable or longer than previous studies.

Development of VLF/LF field strength prediction program using wave-hop theory

*Kenro Nozaki[1], Kuniyasu Imamura[1], Shigeru Tsuchiya[1], Kitauchi Hideaki[2]

1.National Institute of Information and Communications Technology, 2.Kitauchi Lab.

A numerical calculation program for VLF/LF radio wave field strength by means of wave-hop theory adopting the recommendations of the International Telecommunication Union Radiocommunications Sector (ITU-R). The electric field at the receiving point consists of a ground wave and sky waves of from 1-hop to 10-hop modes reflected between the ground and bottom of the ionosphere. Parameters at every ground and ionospheric reflection point are calculated for given day, time, transmitting power, transmitting/receiving location within 16000km. A detailed calculation algorithm and some characteristic results are presented.

Keywords: VLF/LF, field strength, wave-hop theory

